

Top-Quark FCNC Decay $t \rightarrow cgg$ in Topcolor-assisted Technicolor Model

Huan-Jun Zhang

Department of Physics, Henan Normal University, Xinxiang, Henan 453007, China

Abstract

The topcolor-assisted technicolor (TC2) model predicts several pseudo-scalars called top-pions and at loop level they can induce the FCNC top quark decay $t \rightarrow cgg$ which is extremely suppressed in the Standard Model (SM). We find that in the allowed parameter space the TC2 model can greatly enhance such a FCNC decay and push the branching ratio up to 10^{-3} , which is much larger than the predictions in the SM (10^{-9}) and in the minimal supersymmetric model (10^{-4}). We also compare the result with the two-body FCNC decay $t \rightarrow cg$ and find that the braching ratio of $t \rightarrow cgg$ is slightly larger than $t \rightarrow cg$. Such enhanced FCNC top quark decays may serve as a good probe of TC2 model at the future top quark factory.

PACS numbers: 14.65.Ha, 12.60.Fr, 12.60.Jv

Introduction: The upcoming Large Hadron Collider (LHC) will put various new physics ideas to the sword. While this machine has enough energy to produce TeV-scale new particles and thus can directly probe TeV-scale new physics, one should also pay sufficient attention to the indirect probe through revealing quantum effects of new physics in some sensitive processes. As the heaviest fermion in the Standard Model (SM), the top quark is speculated to be a sensitive probe of new physics [1]. So far the top quark properties are not precisely measured due to the small statistics of the experiments at the Fermilab Tevatron collider. The LHC and the proposed International Linear Collider (ILC) will copiously produce top quarks and allow to scrutinize the top quark nature.

One of the properties of the top quark in the SM is its extremely small flavor-changing neutral-current (FCNC) interactions [2] due to the Glashow-Iliopoulos-Maiani (GIM) mechanism. This will make the observation of any FCNC top quark process a robust evidence for new physics beyond the SM. So far numerous studies [3] have shown that the FCNC top quark interactions can be significantly enhanced in some new physics models like the minimal supersymmetric model (MSSM) [4, 5, 6] and the TC2 model [7, 8]. It was found that for these FCNC top quark processes the TC2 model usually allows for much larger production or decay rates than the supersymmetric model. Through the measurements of the FCNC top quark processes at the LHC or ILC, the effects of these new physics models will be revealed.

Although so far in the literature there are several works devoted to the TC2 contributions to the FCNC top quark decays, the TC2 prediction for the three-body decay $t \rightarrow cgg$ has not been studied yet. As shown in [2, 4], in both the SM and MSSM this decay is found to have a larger branching ratio than the two-body decay $t \rightarrow cg$ and thus may be the most hopeful FCNC top decay channel to discover at the LHC or ILC. In this work we focus on the TC2 contribution to this decay and compare its branching ratio with $t \rightarrow cg$.

This work is organized as follows. We will first discuss the TC2 model and then perform the calculations. Since the calculations involve many loops and are somewhat tedious, we will not present the details and will instead give the analytical results in an appendix. We will present some numerical examples with comparison to the results in the SM and MSSM, and finally give our conclusion.

Calculations: Before our calculations we recapitulate the basics of the TC2 model.

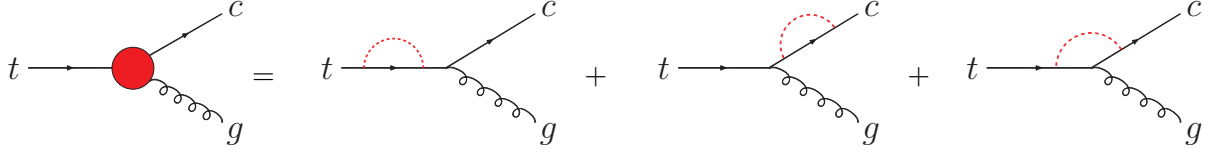


FIG. 1: Feynman diagrams for the effective vertex $t\bar{c}g$ at one-loop level in TC2 model. The boson in each loop denotes a neutral top-pion, a top-Higgs or a charged top-pion, while the fermion in each loop is correspondingly a top or bottom quark.

As is well known, the fancy idea of technicolor aims to dynamically break the electroweak symmetry, but it encounters enormous difficulty in generating fermion masses, especially the heavy top quark mass. The TC2 model [9] combines technicolor with top-color, with the former being responsible for electroweak symmetry breaking and the latter for generating large top-quark mass. This model so far survives current experiments and awaits being tested at the LHC.

A crucial aspect of TC2 phenomenology will be related to the light pseudo-Goldstone bosons called the top-pions (π_t^0 and π_t^\pm), which are predicted in TC2 model at the weak scale [9] and have flavor-changing couplings with the top quark

$$\begin{aligned} \frac{(1-\epsilon)m_t}{\sqrt{2}F_t} \frac{\sqrt{v^2 - F_t^2}}{v} & \left(iK_{UL}^{tt}K_{UR}^{tt}\bar{t}_L t_R \pi_t^0 + iK_{UL}^{tt}K_{UR}^{tc}\bar{t}_L c_R \pi_t^0 \right. \\ & + \sqrt{2}K_{UR}^{tt}K_{DL}^{bb}\bar{t}_R b_L \pi_t^- + \sqrt{2}K_{UR}^{tc}K_{DL}^{bb}\bar{c}_R b_L \pi_t^- \\ & \left. + K_{UL}^{tt}K_{UR}^{tt}\bar{t}_L t_R h_t^0 + K_{UL}^{tt}K_{UR}^{tc}\bar{t}_L c_R h_t^0 + h.c. \right), \end{aligned} \quad (1)$$

where the factor $\sqrt{v^2 - F_t^2}/v$ ($v \simeq 174$ GeV) reflects the effect of the mixing between the top pions and the would-be Goldstone bosons. The parameter ϵ parameterizes the portion of the extended-technicolor contribution to the top quark mass. K_{UL}, K_{DL} and K_{UR} are the rotation matrices that transform respectively the weak eigenstates of left-handed up-type, down-type, and right-handed up-type quarks to their mass eigenstates, whose values can be parameterized as [8]

$$K_{UL}^{tt} \simeq 1, \quad K_{UR}^{tt} \simeq \frac{m_t'}{m_t} = 1 - \epsilon, \quad K_{UR}^{tc} \leq \sqrt{1 - (K_{UR}^{tt})^2} = \sqrt{2\epsilon - \epsilon^2}, \quad (2)$$

with m_t' denoting the top-color contribution to the top quark mass. In our calculations we assume $K_{UR}^{tc} = \sqrt{1 - (K_{UR}^{tt})^2}$. The TC2 model also predicts a CP-even scalar called top Higgs (h_t^0) whose couplings to top quark are similar to the neutral top pion [8].

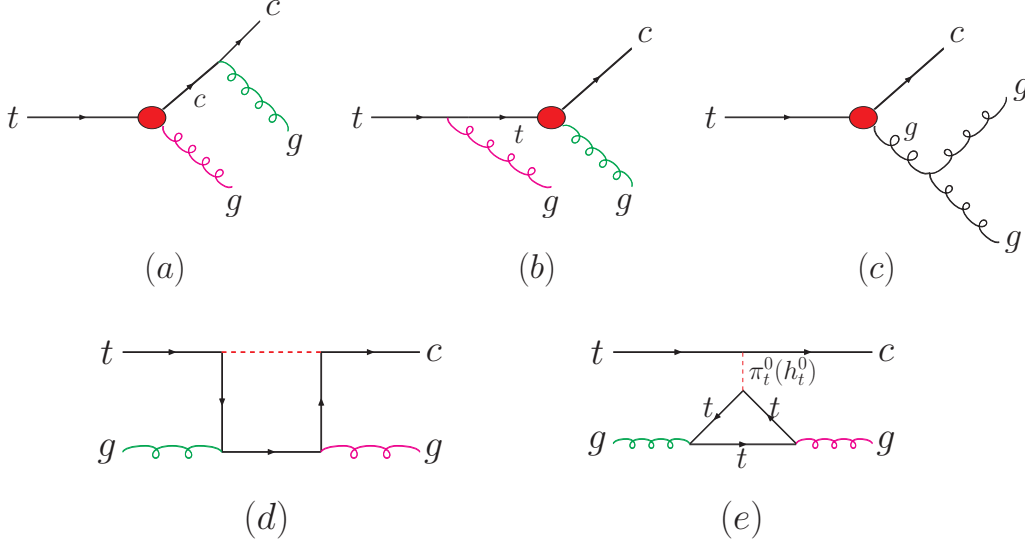


FIG. 2: Feynman diagrams for $t \rightarrow cgg$ at one-loop level in TC2 model. The effective vertex $t\bar{c}g$ in (a-c) is defined in Fig. 1. The boson in the loop of the box diagram (d) can be a neutral top-pion, top-Higgs or a charged top-pion, while the fermion in the loop can be a top or bottom quark correspondingly. The two gluons in (a,b,d,e) can be exchanged.

These flavor-changing couplings will induce the FCNC coupling $t\bar{c}g$, as shown in Fig. 1. We follow the idea of the 'effective vertex' in [4] and define an effective $t\bar{c}g$ vertex to simplify our calculations

$$\Gamma_{\mu}^{eff}(p_t, p_c) = \Gamma_{\mu}^{t\bar{c}g}(p_t, p_c) + \Gamma_{\mu}^{c\bar{c}g} \frac{i(\not{p}_t + m_c)}{p_t^2 - m_c^2} i\Sigma(p_t) + i\Sigma(p_c) \frac{i(\not{p}_c + m_t)}{p_c^2 - m_t^2} \Gamma_{\mu}^{t\bar{t}g}, \quad (3)$$

where $\Gamma_{\mu}^{q\bar{q}g}$ ($q = c, t$) is the usual QCD vertex, and $\Gamma_{\mu}^{t\bar{c}g}$, $\Sigma(p_t)$ and $\Sigma(p_c)$ are respectively the contributions from vertex and self-energy loops shown in Fig. 1, whose expressions are given in the Appendix. Such an effective vertex can be re-shaped in the form

$$F_1(k^2)T^a(k^2\gamma_{\mu} - k_{\mu}\not{k}) + m_t F_2(k^2)T^a i\sigma_{\mu\nu}k^{\nu}, \quad (4)$$

where k denotes the momentum of the gluon, T^a ($a = 1, \dots, 8$) are the $SU_c(3)$ generators, and $F_{1,2}(k^2)$ are form factors arising from loop calculations. Note that for the two-body decay $t \rightarrow cg$, F_1 does not contribute since the gluon momentum k satisfies $k^2 = 0$ and $k \cdot \epsilon = 0$ with ϵ being the gluon polarization vector (different from ϵ in Eqs.(1) and (2) !).

With the effective vertex defined above, the Feynman diagrams for the decay $t \rightarrow cgg$ are shown in Fig. 2, where the diagrams (a-c) involve the effective vertex. The amplitudes of the diagrams (a-c) are obvious with the defined effective vertex. In addition, we need

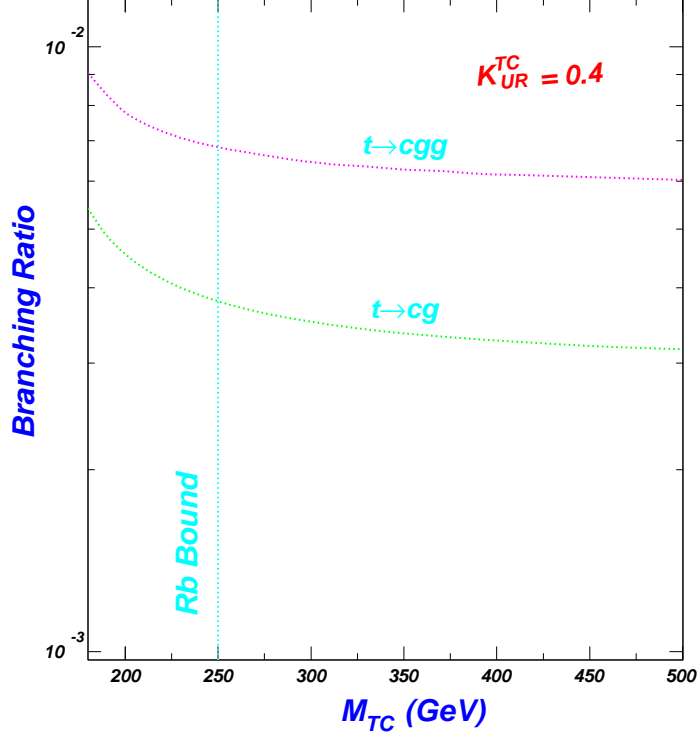


FIG. 3: Branching ratios of $t \rightarrow cgg$ and $t \rightarrow cg$ versus M_{TC} in TC2 model.

to calculate the box diagrams shown in Fig.2(d) and the triangle top-quark loop diagram shown in Fig.2(e). The calculations are straightforward and the results are given in the Appendix.

Numerical results: Now we are ready to give some numerical results. First, we take a look at the involved parameters. The parameters in our calculations are the masses of the top-pions and top-Higgs, K_{UR}^{TC} , and the top-pion decay constant F_t . In our calculations we take $m_t = 170.9$ GeV [10] and $F_t = 50$ GeV. About the top-pion and top-Higgs masses, in our analysis we assume

$$m_{\pi_t^0} = m_{\pi_t^\pm} = m_{h_t^0} \equiv M_{TC} \quad (5)$$

In our figures of numerical results we will show a bound of about 250 GeV on top-pion mass, which is from R_b constraint on the charged top-pion [11]. Note that such a bound is not so robust since in TC2 model the sizable corrections to R_b can also come from the extended technicolor gauge bosons.

In our numerical results we give the branching ratio with the top width taken to be $\Gamma_t = 1.55$ GeV [6]. To make our predictions more realistic, we apply some kinematic cuts as in [4], e.g., we require the energy of each decay product be larger than 15 GeV in the top

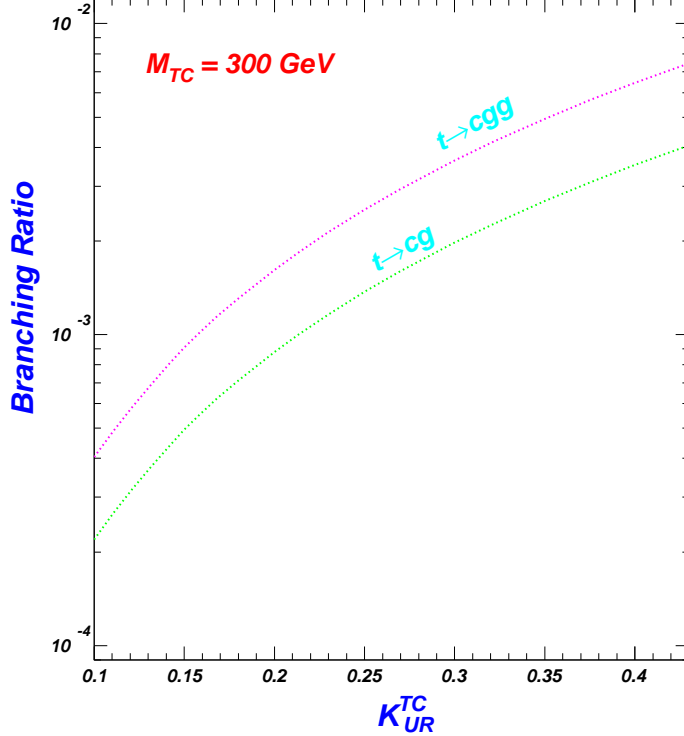


FIG. 4: Branching ratios of $t \rightarrow cgg$ and $t \rightarrow cg$ versus K_{UR}^{TC} in TC2 model.

quark rest frame.

In Fig.3 we show the branching ratios of $t \rightarrow cgg$ and $t \rightarrow cg$ versus M_{TC} . We see that the contributions of top-pions can significantly enhance such rare decays and in the allowed parameter space the branching ratio can be up to 10^{-3} , which is much larger than the predictions in the SM (10^{-9}) [2] and in the MSSM (10^{-4}) [4].

As shown in Fig.3, the branching ratio of $t \rightarrow cgg$ is larger than $t \rightarrow cg$, which is also observed in the SM [2] and the MSSM [4]. As discussed in [2, 4], the reason for this behavior is that the form factor F_1 in Eq.(4), which makes important contribution to $t \rightarrow cgg$, does not contribute to $t \rightarrow cg$.

Note that the TC2 contributions are sensitive to the parameter K_{UR}^{TC} which is fixed to 0.4 in Fig.3. In Fig.4 we show the dependence on K_{UR}^{TC} for fixed top-pion mass. We see that the branching ratios increase drastically as K_{UR}^{TC} gets large.

Finally, in Table 1 we summarize the TC2 predictions for the FCNC top quark decays with comparison to the predictions in the SM and MSSM. The TC2 predictions are taken from Fig.3 for $M_{TC} = 300$ GeV and $K_{UR}^{TC} = 0.4$. We see that for each decay mode the TC2 model allows a much larger branching ratio than the other two models.

Table 1: Predictions for the branching ratios of the FCNC top quark decays. The TC2 predictions are taken from Fig.3 for $M_{TC} = 300$ GeV and $K_{UR}^{TC} = 0.4$. The MSSM predictions are the maximal values in the allowed parameter space.

| | SM | MSSM | TC2 |
|-----------------------------|------------------|-----------------|-----------------|
| $Br(t \rightarrow cZ)$ | $O(10^{-13})[2]$ | $O(10^{-7})[4]$ | $O(10^{-4})[7]$ |
| $Br(t \rightarrow c\gamma)$ | $O(10^{-13})[2]$ | $O(10^{-7})[4]$ | $O(10^{-6})[7]$ |
| $Br(t \rightarrow cg)$ | $O(10^{-11})[2]$ | $O(10^{-5})[4]$ | $O(10^{-3})$ |
| $Br(t \rightarrow cgg)$ | $O(10^{-9})[2]$ | $O(10^{-4})[4]$ | $O(10^{-3})$ |

In conclusion, we evaluated the TC2 contributions to the top quark FCNC decay $t \rightarrow cgg$ with comparison to $t \rightarrow cg$. We found that the branching ratios for these two decays can be enhanced to the level of 10^{-3} , which is much larger than the predictions in both the SM and MSSM. As in the SM and MSSM, the decay $t \rightarrow cgg$ was found to have a larger branching ratio than two-body decay $t \rightarrow cg$. The future precision study of the top quark properties at the LHC or ILC, especially the measurement of various rare decay modes, will shed some light on the TC2 model.

We thank Junjie Cao, Jin Min Yang and Xuelei Wang for discussions, and Wenyu Wang and Lei Wang for help with the fortran codes.

APPENDIX A: EXPRESSIONS OF LOOP RESULTS

The expressions of $\Gamma_\mu^{t\bar{c}g}$, $\Sigma(p_t)$ and $\Sigma(p_c)$ in the effective vertex of Eq.(3) are given by

$$\begin{aligned} \Gamma_\mu^{t\bar{c}g} = & \frac{1}{2}ag_s^2P_L [\gamma^\rho\gamma^\mu\gamma^\lambda(C_{\rho\lambda}^1 + C_{\rho\lambda}^2 + 2C_{\rho\lambda}^3) + \gamma^\rho\gamma^\mu\not{k}(C_\rho^1 + C_\rho^2 + 2C_\rho^3) \\ & + m_t\gamma^\rho\gamma^\mu(-C_\rho^1 + C_\rho^2) + m_t\gamma^\mu\gamma^\rho(-C_\rho^1 + C_\rho^2) + m_t\gamma^\mu\not{k}(-C_0^1 + C_0^2) \\ & + m_t^2\gamma^\mu(-C_0^1 + C_0^2)] \end{aligned} \quad (A1)$$

$$i\Sigma(p_t) = \frac{1}{2}aP_L[\not{p}'_t(B_1^1 + B_1^2 + 2B_1^3) + m_t(-B_0^1 + B_0^2)] \quad (A2)$$

$$i\Sigma(p_c) = \frac{1}{2}aP_L[\not{p}'_c(B_1^4 + B_1^5 + 2B_1^6) + m_t(-B_0^4 + B_0^5)] \quad (A3)$$

with p_t , p_c and k denoting respectively the momenta of the top, charm quark and gluon, $a = \frac{m_t^2}{F_t^2} \frac{v^2 - F_t^2}{v^2} K_{UR}^{TC}$ and the loop functions' dependence given by

$$B^1 = B(p_t^2, m_t^2, m_{\pi_t^0}^2), \quad B^2 = B(p_t^2, m_t^2, m_{h_t^0}^2), \quad B^3 = B(p_t^2, m_b^2, m_{\pi_t^+}^2), \quad (\text{A4})$$

$$B^4 = B(p_c^2, m_t^2, m_{\pi_t^0}^2), \quad B^5 = B(p_c^2, m_t^2, m_{h_t^0}^2), \quad B^6 = B(p_c^2, m_b^2, m_{\pi_t^+}^2), \quad (\text{A5})$$

$$C^1 = C(k, -p_t, m_t^2, m_t^2, m_{\pi_t^0}^2), \quad C^2 = C(k, -p_t, m_t^2, m_t^2, m_{h_t^0}^2), \quad (\text{A6})$$

$$C^3 = C(k, -p_t, m_b^2, m_b^2, m_{\pi_t^+}^2) \quad (\text{A7})$$

The amplitudes of the box diagrams in Fig.2(d) is given by

$$\begin{aligned} M_1 = & -\frac{1}{2} a g_s^2 T_1 \frac{i}{16\pi^2} \bar{u}(p_c) P_L \{ -\gamma^\rho \gamma^\nu \gamma^\lambda \gamma^\mu \gamma^\sigma D_{\rho\lambda\sigma}^1 - \gamma^\rho \gamma^\nu \gamma^\lambda \gamma^\mu \not{p}_1 D_{\rho\lambda}^1 - \gamma^\rho \gamma^\nu \gamma^\lambda \gamma^\mu \not{p}_2 D_{\rho\lambda}^1 \\ & + m_t \gamma^\rho \gamma^\nu \gamma^\lambda \gamma^\mu D_{\rho\lambda}^1 - \gamma^\rho \gamma^\nu \not{p}_2 \gamma^\mu \gamma^\lambda D_{\rho\lambda}^1 + m_t \gamma^\rho \gamma^\nu \gamma^\mu \gamma^\lambda D_{\rho\lambda}^1 \\ & - \gamma^\rho \gamma^\nu \not{p}_2 \gamma^\mu \not{p}_2 D_\rho^1 + m_t \gamma^\rho \gamma^\nu \not{p}_2 \gamma^\mu D_\rho^1 - \gamma^\rho \gamma^\nu \not{p}_2 \gamma^\mu \not{p}_1 D_\rho^1 \\ & + m_t \gamma^\rho \gamma^\nu \gamma^\mu \not{p}_1 D_\rho^1 + m_t \gamma^\rho \gamma^\nu \gamma^\mu \not{p}_2 D_\rho^1 + m_t \gamma^\nu \not{p}_2 \gamma^\mu \not{p}_2 D_0^1 \\ & + m_t \gamma^\nu \gamma^\rho \gamma^\mu \gamma^\lambda D_{\rho\lambda}^1 + m_t \gamma^\nu \gamma^\rho \gamma^\mu \not{p}_1 D_\rho^1 + m_t \gamma^\nu \gamma^\rho \gamma^\mu \not{p}_2 D_\rho^1 \\ & - m_t^2 \gamma^\nu \gamma^\rho \gamma^\mu D_\rho^1 + m_t \gamma^\nu \not{p}_2 \gamma^\mu \gamma^\rho D_\rho^1 + m_t \gamma^\nu \not{p}_2 \gamma^\mu \not{p}_1 D_0^1 \\ & - m_t^2 \gamma^\rho \gamma^\nu \gamma^\mu D_\rho^1 - m_t^2 \gamma^\nu \not{p}_2 \gamma^\mu D_0^1 - m_t^2 \gamma^\nu \gamma^\mu \gamma^\rho D_\rho^1 \\ & - m_t^2 \gamma^\nu \gamma^\mu \not{p}_1 D_0^1 - m_t^2 \gamma^\nu \gamma^\mu \not{p}_2 D_0^1 + m_t^3 \gamma^\nu \gamma^\mu D_0^1 \} u(p_t) \epsilon_\nu^*(p_2) \epsilon_\mu^*(p_1) \quad (\text{A8}) \end{aligned}$$

$$\begin{aligned} M_2 = & \frac{1}{2} a g_s^2 T_1 \frac{i}{16\pi^2} \bar{u}(p_c) P_L \{ \gamma^\rho \gamma^\nu \gamma^\lambda \gamma^\mu \gamma^\sigma D_{\rho\lambda\sigma}^2 + \gamma^\rho \gamma^\nu \gamma^\lambda \gamma^\mu \not{p}_2 D_{\rho\lambda}^2 + \gamma^\rho \gamma^\nu \gamma^\lambda \gamma^\mu \not{p}_2 D_{\rho\lambda}^2 \\ & + m_t \gamma^\rho \gamma^\nu \gamma^\lambda \gamma^\mu D_{\rho\lambda}^2 + \gamma^\rho \gamma^\nu \not{p}_2 \gamma^\mu \gamma^\lambda D_{\rho\lambda}^2 + m_t \gamma^\rho \gamma^\nu \gamma^\mu \gamma^\lambda D_{\rho\lambda}^2 \\ & + \gamma^\rho \gamma^\nu \not{p}_2 \gamma^\mu \not{p}_2 D_\rho^2 + m_t \gamma^\rho \gamma^\nu \not{p}_2 \gamma^\mu D_\rho^2 + \gamma^\rho \gamma^\nu \not{p}_2 \gamma^\mu \not{p}_1 D_\rho^2 \\ & + m_t \gamma^\rho \gamma^\nu \gamma^\mu \not{p}_1 D_\rho^2 + m_t \gamma^\rho \gamma^\nu \gamma^\mu \not{p}_2 D_\rho^2 + m_t \gamma^\nu \not{p}_2 \gamma^\mu \not{p}_2 D_0^2 \\ & + m_t \gamma^\nu \gamma^\rho \gamma^\mu \gamma^\lambda D_{\rho\lambda}^2 + m_t \gamma^\nu \gamma^\rho \gamma^\mu \not{p}_1 D_\rho^2 + m_t \gamma^\nu \gamma^\rho \gamma^\mu \not{p}_2 D_\rho^2 \\ & + m_t^2 \gamma^\nu \gamma^\rho \gamma^\mu D_\rho^2 + m_t \gamma^\nu \not{p}_2 \gamma^\mu \gamma^\rho D_\rho^2 + m_t \gamma^\nu \not{p}_2 \gamma^\mu \not{p}_1 D_0^2 \\ & + m_t^2 \gamma^\rho \gamma^\nu \gamma^\mu D_\rho^2 + m_t^2 \gamma^\nu \not{p}_2 \gamma^\mu D_0^2 + m_t^2 \gamma^\nu \gamma^\mu \gamma^\rho D_\rho^2 \\ & + m_t^2 \gamma^\nu \gamma^\mu \not{p}_1 D_0^2 + m_t^2 \gamma^\nu \gamma^\mu \not{p}_2 D_0^2 + m_t^3 \gamma^\nu \gamma^\mu D_0^2 \} u(p_t) \epsilon_\nu^*(p_2) \epsilon_\mu^*(p_1) \quad (\text{A9}) \end{aligned}$$

$$\begin{aligned} M_3 = & a g_s^2 T_1 \frac{i}{16\pi^2} \bar{u}(p_c) P_L \{ \gamma^\rho \gamma^\nu \gamma^\lambda \gamma^\mu \gamma^\sigma D_{\rho\lambda\sigma}^3 + \gamma^\rho \gamma^\nu \gamma^\lambda \gamma^\mu \not{p}_2 D_{\rho\lambda}^3 + \gamma^\rho \gamma^\nu \gamma^\lambda \gamma^\mu \not{p}_2 D_{\rho\lambda}^3 \\ & + m_t \gamma^\rho \gamma^\nu \gamma^\lambda \gamma^\mu D_{\rho\lambda}^3 + \gamma^\rho \gamma^\nu \not{p}_2 \gamma^\mu \not{p}_2 D_\rho^3 + \gamma^\rho \gamma^\nu \not{p}_2 \gamma^\mu \not{p}_1 D_\rho^3 \} u(p_t) \epsilon_\nu^*(p_2) \epsilon_\mu^*(p_1) \quad (\text{A10}) \end{aligned}$$

with $T_1 = T_{nm}^b T_{ml}^a$ (n, l, a, b are respectively the color indices of the top, charm quark and the two gluons), p_1 and p_2 denoting the momenta of the two gluons, and the four-piont loop

functions' dependence given by

$$D^1 = D^1(p_2, p_1, -p_t, m_t, m_t, m_{\pi_t^0}) \quad (\text{A11})$$

$$D^2 = D^2(p_2, p_1, -p_t, m_t, m_t, m_{h_t^0}) \quad (\text{A12})$$

$$D^3 = D^3(p_2, p_1, -p_t, m_b, m_b, m_{\pi_t^+}) \quad (\text{A13})$$

The amplitudes of the top-quark triangle loop digrams in Fig.2(e) are given by

$$M_1 = \frac{1}{2} a g_s^2 T_2 \frac{i}{16\pi^2} \frac{i}{(p_1 + p_2)^2 - m_{\pi_t^0}^2} 4m_t \bar{u}_c P_R \varepsilon^{\rho\lambda\nu\mu} p_{2\rho} p_{1\lambda} C_0 \bar{u}_t \epsilon_\nu^*(p_2) \epsilon_\mu^*(p_1) \quad (\text{A14})$$

$$M_2 = -\frac{1}{2} a g_s^2 T_2 \frac{i}{16\pi^2} \frac{i}{(p_1 + p_2)^2 - m_{\pi_t^0}^2} \bar{u}_c P_L m_t \{ -4g_{\mu\nu} B_0 - 16p_{1\nu} C_\mu + 16C_{\mu\nu} + 8p_1^\alpha C_\alpha g_{\mu\nu} - 4p_1^2 g_{\mu\nu} C_0 - 4p_1 \cdot p_2 g_{\mu\nu} C_0 + 4p_{1\nu} p_{2\mu} C_0 \} \bar{u}_t \epsilon_\nu^*(p_2) \epsilon_\mu^*(p_1) \quad (\text{A15})$$

with $T_2 = T_{nm}^b T_{ml}^a$ and the loop functions' dependence given by

$$B = B(p_2^2, m_t^2, m_t^2), \quad C = C(-p_1, -p_2, m_t, m_t, m_t). \quad (\text{A16})$$

In the above expressions the loop functions B , C and D with Lorentz indices can be expanded into scalar functions [12], which can be calculated by using LoopTools [13].

-
- [1] See, e.g., D. Chakraborty, J. Konigsberg, D. Rainwater, *Ann. Rev. Nucl. Part. Sci.* **53**, 301 (2003); E. H. Simmons, hep-ph/0211335; C.-P. Yuan, hep-ph/0203088; S. Willenbrock, hep-ph/0211067; M. Beneke *et al.*, hep-ph/0003033; C. T. Hill and S. J. Parke, *Phys. Rev. D* **49**, 4454 (1994); K. Whisnant, et al., *Phys. Rev. D* **56**, 467 (1997); K. Hikasa, et al., *Phys. Rev. D* **58**, 114003 (1998).
- [2] For the FCNC top quark decays in the SM, see, G. Eilam, J. L. Hewett and A. Soni, *Phys. Rev. D* **44**, 1473 (1991); B. Mele, S. Petrarca and A. Soddu, *Phys. Lett. B* **435**, 401 (1998); A. Cordero-Cid, *et al.*, *Phys. Rev. D* **73**, 094005 (2006); G. Eilam, M. Frank and I. Turan, *Phys. Rev. D* **73**, 053011 (2006).
- [3] For recent reviews, see, e.g., F. Larios, R. Martinez, M. A. Perez, *Int. J. Mod. Phys. A* **21**, 3473 (2006); J. M. Yang, *Annals Phys.* **316**, 529 (2005).
- [4] For the latest results of MSSM predictions for FCNC top decays and productions at LHC, see, J. Cao, *et. al.*, *Phys. Rev. D* **75**, 075021 (2007); *Phys. Rev. D* **74**, 031701 (2006).

- [5] For earlier studies on FCNC top decays in the MSSM, see, C. S. Li, R. J. Oakes and J. M. Yang, Phys. Rev. D **49**, 293 (1994); G. Couture, C. Hamzaoui and H. Konig, Phys. Rev. D **52**, 1713 (1995); J. L. Lopez, D. V. Nanopoulos and R. Rangarajan, Phys. Rev. D **56**, 3100 (1997); G. M. de Divitiis, R. Petronzio and L. Silvestrini, Nucl. Phys. B **504**, 45 (1997); J. M. Yang, B.-L. Young and X. Zhang, Phys. Rev. D **58**, 055001 (1998); C. S. Li, L. L. Yang and L. G. Jin, Phys. Lett. B **599**, 92 (2004); M. Frank and I. Turan, Phys. Rev. D **74**, 073014 (2006); J. M. Yang and C. S. Li, Phys. Rev. D **49**, 3412 (1994); J. Guasch and J. Sola, Nucl. Phys. B **562**, 3 (1999); G. Eilam, *et al.*, Phys. Lett. B **510**, 227 (2001). J.L. Diaz-Cruz, H.-J. He, C.-P. Yuan Phys. Lett. B **179**,530 (2002); D. Delepine and S. Khalil, Phys. Lett. B **599**, 62 (2004).
- [6] Other works on top FCNC productions in the MSSM: J. Cao, Z. Xiong, J.M.Yang, Nucl. Phys. B **651**, 87 (2003); J. J. Liu, C. S. Li, L. L. Yang and L. G. Jin, Nucl. Phys. B **705**, 3 (2005); G. Eilam, M. Frank and I. Turan, Phys. Rev. D **74**, 035012 (2006); J. Guasch, *et al.*, Nucl. Phys. Proc. Suppl. 157, 152 (2006); D. Lopez-Val, J. Guasch, J. Sola, arXiv:0710.0587
- [7] For FCNC top quark decays in TC2 theory, see, X. L. Wang *et al.*, Phys. Rev. D **50**, 5781 (1994); C. Yue, *et al.*, Phys. Rev. D **64**, 095004 (2001); G. Lu, F. Yin, X. Wang and L. Wan, Phys. Rev. D **68**, 015002 (2003).
- [8] For exotic top production processes in TC2 models, see, H. J. He and C. P. Yuan, Phys. Rev. Lett. **83**, 28(1999); G. Burdman, Phys. Rev. Lett. **83**,2888(1999); J. Cao, Z. Xiong, J. M. Yang, Phys. Rev. D **67**, 071701 (2003); C. Yue, *et al.*, Phys. Lett. B **496**, 93 (2000); J. Cao, *et al.*, Phys. Rev. D **70**, 114035 (2004); F. Larios and F. Penunuri, J. Phys. G **30**, 895(2004); J. Cao, *et al.* Eur. Phys. Jour. C **41**, 381 (2005); Phys. Rev. D **76**, 014004 (2007); G. Liu and H. Zhang, arXiv:0708.1553.
- [9] C. T. Hill, Phys. Lett. B **345**, 483 (1995); K. Lane and E. Eichten, Phys. Lett. B **352**, 382 (1995); K. Lane and E. Eichten, Phys. Lett. B **433**, 96 (1998); W. A. Bardeen, C. T. Hill, M. Lindner, Phys. Rev. D **41**, 1647 (1990); G. Cvetič, Rev. Mod. Phys. **71**, 513 (1999).
- [10] Tevatron Electroweak Working Group (for the CDF and D0 Collaborations), hep-ex/0703034.
- [11] C. T. Hill, X. Zhang, Phys. Rev. D **51**, 3563 (1995); C. Yue, Y. P. Kuang, X. Wang, W. Li, Phys. Rev. D **62**, 055005 (2000).
- [12] G. 't Hooft and M. J. G. Veltman, Nucl. Phys. B **153**, 365 (1979).
- [13] T. Hahn, M. Perez-Victoria, Comput. Phys. Commun. **118**, 153 (1999); T. Hahn, Nucl. Phys.

Proc. Suppl. **135**, 333 (2004).